journal

J. Am. Ceram. Soc., **82** [5] 1263–68 (1999)

Elastic Properties and Structure of Interpenetrating Boron Carbide/Aluminum Multiphase Composites

Salvatore Torquato,[†,§] Christofer L. Y. Yeong,[†,§] Mark D. Rintoul,[†,§] David L. Milius,[*,‡,§] and Ilhan A. Aksay[*,‡,§]

Department of Civil Engineering and Operations Research, Department of Chemical Engineering, and Princeton Materials Institute, Princeton University, Princeton, New Jersey, 08544-5263

We study the elastic moduli and structure of boron carbide/aluminum (B_4C/Al) multiphase composites using rigorous bounding and experimental characterization techniques. We demonstrate that rigorous bounds on the effective moduli are useful in that they can accurately predict (i) the effective elastic moduli, given the phase moduli and volume fractions, or (ii) the phase moduli (volume fractions), given the effective moduli and phase volume fractions (moduli). Using the best available rigorous bounds on the effective elastic moduli of multiphase composites involving volume-fraction information, we are able to predict the bulk and shear moduli of the Al_4BC phase, a reaction product that forms during heat treatment. These theoretical predictions are in very good agreement with recent experimental measurements of the moduli of the Al_4BC phase. Moreover, we evaluate more-refined bounds involving three-point structural correlation functions by extracting such information from an image of a sample of the B_4C/Al composite. Although experimental data for the effective moduli are unavailable for this sample, our predictions of the effective moduli based on three-point bounds should be quite accurate.

I. Introduction

THE problem of determining the effective mechanical and transport properties of composite materials has a long history, attracting the attention of such luminaries of science as Maxwell,[1] Rayleigh,[2] and Einstein.[3] Because of its fundamental and technological importance, this problem continues to be the focus of intense research (see the reviews of Refs. 4–8 and the references therein). From a design as well as theoretical point of view, it is desirable to calculate the effective properties from a knowledge of the structure of the composite material; we can then systematically relate changes in the structure quantitatively to changes in the macroscopic parameters. However, an infinite set of correlation functions that statistically characterizes the structure must be known to predict exactly the effective properties.[7,9] Except for a few special cases, the infinite set of correlation functions is never known, and, hence, an exact, analytical determination of the effective properties, for all phase properties and volume fractions, is generally intractable, even for simple random models (e.g., random arrays of oriented cylinders or of spheres). Therefore, we usually resort to obtaining solutions for idealized geometries (e.g., periodic arrays of spheres in matrix[10]), finding approximate solutions (such as popular self-consistent formulas[11,12]), or obtaining rigorous bounds on the effective properties for the actual microstructure, given limited information about it.[7,13–23] Clearly, idealized models are severely limited in their applicability, and approximate, self-consistent formulas typically involve crude structural information (e.g., volume fractions and inclusion shapes) and, thus, are not good approximations for a wide class of materials. On the other hand, bounding techniques have proved to be fruitful, because the bounds can yield useful estimates of the properties, even when the bounds diverge from one another in the strong-contrast limit.[7]

The preponderance of the aforementioned work has been conducted for two-phase composite materials, and, within this category, much of the research has focused on those materials comprised of well-defined inclusions (e.g., spheres and cylinders) in a connected matrix (see Fig. 1(a)). The reason is that it is much more difficult to treat two-phase composites in which both phases are connected, i.e., interpenetrating two-phase composites (see Fig. 1(b)). Much less work has been performed for multiphase composites, especially as it regards comparing theoretical property estimates to experimental data.

This paper begins a program to study, both theoretically and experimentally, the mechanical properties of multiphase materials using rigorous bounding methods, Monte Carlo techniques, and experimental characterization techniques. Here, we specifically work with boron carbide/aluminum (B_4C/Al) interpenetrating composites that we have fabricated by a process described elsewhere.[24–26]

The paper is organized as follows: in Section II, we give an overview of rigorous bounds for composites; in Section III, we describe our analyses of the elastic moduli of the B_4C/Al composites; and in Section IV, we make concluding remarks.

II. Overview of Rigorous Bounds

Here we review briefly rigorous bounds on the effective elastic moduli of composite media. The reader is referred to the article by Torquato[7] for a comprehensive review of this subject. We generally consider a macroscopically isotropic composite composed of N isotropic phases. Let K_i and G_i be the bulk and shear moduli, respectively, of the ith phase and ϕ_i the corresponding volume fraction. Moreover, we denote by K_e and G_e the effective bulk modulus and effective shear modulus, respectively, of an isotropic composite.

(1) One-Point Bounds

One of the simplest set of bounds on K_e and G_e is the so-called Voigt–Reuss bounds given by

$$\left\langle \frac{1}{K} \right\rangle^{-1} \leq K_e \leq \langle K \rangle \tag{1}$$

$$\left\langle \frac{1}{G} \right\rangle^{-1} \leq G_e \leq \langle G \rangle \tag{2}$$

B. N. Cox—contributing editor

Manuscript No. 190688. Received September 20, 1997; approved August 24, 1998.
*Member, American Ceramic Society.
†Department of Civil Engineering and Operations Research.
‡Department of Chemical Engineering.
§Princeton Materials Institute.

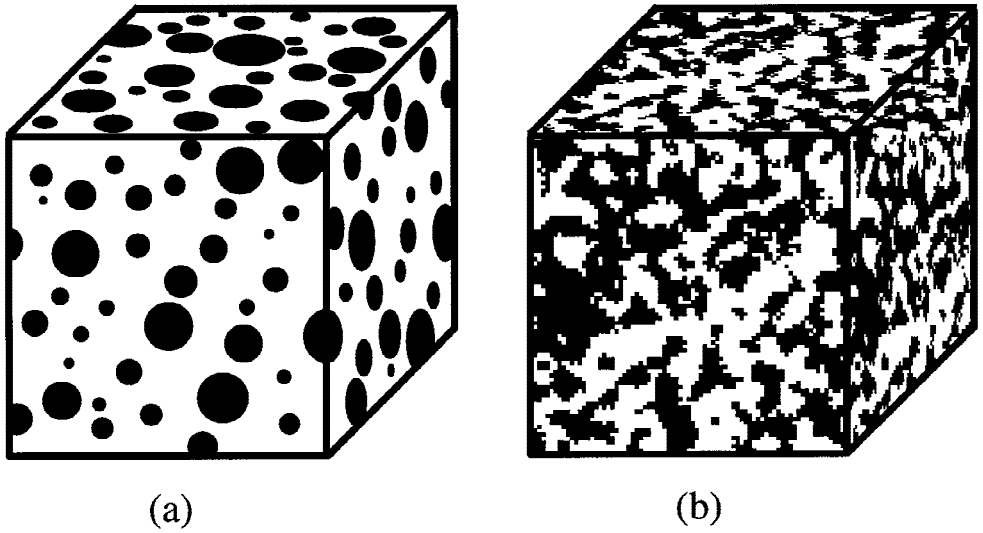

Fig. 1. Schematic of (a) a particulate composite and (b) an interpenetrating two-phase composite. Particulate composite consists of nonoverlapping, disconnected particles in a connected matrix. Interpenetrating composite consists of two connected phases.

where $\langle b \rangle$ and $\langle 1/b \rangle^{-1}$ are simply the arithmetic and harmonic averages, respectively, of the phase moduli, which are defined for an arbitrary property b by

$$\langle b \rangle = \sum_{i=1}^{N} \phi_i b_i \tag{3a}$$

$$\left\langle \frac{1}{b} \right\rangle = \sum_{i=1}^{N} \frac{\phi_i}{b_i} \tag{3b}$$

Bounds in Eqs. (1) and (2) have been proved, respectively, by Hill[13] and Paul.[14] They are easily obtained from minimum energy principles by taking the admissible strain and stress fields to be constant tensors. We refer to Eqs. (1) and (2) as *one-point* bounds, because they involve only phase volume-fraction information. Observe that ϕ_i is a one-point correlation function, because it is equivalent to the probability of finding a point (when randomly inserted into the composite) in phase i.

(2) Two-Point Bounds

Hashin and Shtrikman (HS)[15] used "polarization" variational principles to obtain two-point bounds on K_e and G_e for two-phase isotropic composites. We refer to these as two-point bounds, because they depend on an integral involving the two-point probability function $S_2(r)$, which gives the probability that two points, separated by a distance r, lie in one of the phases, say phase 1 (see Fig. 2). However, this integral depends only on the extreme values of $S_2(r)$ and, hence, is expressible simply in terms of the volume fractions ϕ_1 and ϕ_2. The HS bounds for two-phase composites when $K_2 \geq K_1$ and $G_2 \geq G_1$ are given by

$$\langle K \rangle - \frac{\phi_1 \phi_2 (K_2 - K_1)^2}{\langle \tilde{K} \rangle + \frac{4}{3} G_1} \leq K_e \leq \langle K \rangle - \frac{\phi_1 \phi_2 (K_2 - K_1)^2}{\langle \tilde{K} \rangle + \frac{4}{3} G_2} \tag{4}$$

$$\langle G \rangle - \frac{\phi_1 \phi_2 (G_2 - G_1)^2}{\langle \tilde{G} \rangle + G_1 \left[\frac{9K_1 + 8G_1}{6(K_1 + 2G_1)} \right]} \leq G_e \leq \langle G \rangle - \frac{\phi_1 \phi_2 (G_2 - G_1)^2}{\langle \tilde{G} \rangle + G_2 \left[\frac{9K_2 + 8G_2}{6(K_2 + 2G_2)} \right]} \tag{5}$$

$$\langle \tilde{b} \rangle = \phi_1 b_2 + \phi_2 b_1 \tag{6}$$

The HS bounds are realizable (exact) for certain types of dispersions and, therefore, represent the optimal (best possible) bounds on the effective elastic moduli, given only volume-fraction information. In the case of K_e, the HS bounds are achieved by coated-sphere assemblages, shown in Fig. 3. The HS lower bound corresponds to coated spheres consisting of a core of the stiffer material (phase 2) with radius R_c, surrounded by a concentric shell of the more compliant material (phase 1) with outer radius R_o. The ratio $(R_c/R_o)^3 = \phi_2$, and the coated spheres fill all of space, implying that there is a distribution in their sizes ranging to the infinitesimally small. The stiffer phase is always disconnected (except in the trivial instance when $\phi_2 = 1$). As far as K_e is concerned, the HS lower bound construction can be regarded as the most "disconnected" arrangement of the stiffer material, because phase 2 elements are well separated from each other. The HS upper bound corresponds to the aforementioned coated-sphere assemblage but with phase 1 interchanged with phase 2. Thus, for the upper bound geometry, the stiffer phase is always connected (except in the trivial case when $\phi_2 = 0$) and, hence, can be regarded as the most "connected" arrangement of the stiffer material. Similarly, the HS bounds on G_e are exact for certain hierarchical laminates;[27–28] the HS bounds are not attained by coated-sphere assemblages, however. Again, the laminates have the same connectivity properties as the coated-sphere assemblages; i.e., the lower bound structure corresponds to one in which the stiffer phase is the dispersed phase, whereas the upper bound structure corresponds to one in which the stiffer phase is con-

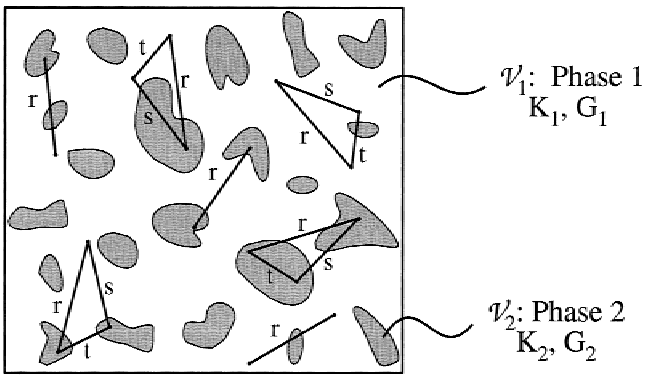

Fig. 2. Schematic interpretation of the two- and three-point correlation functions.

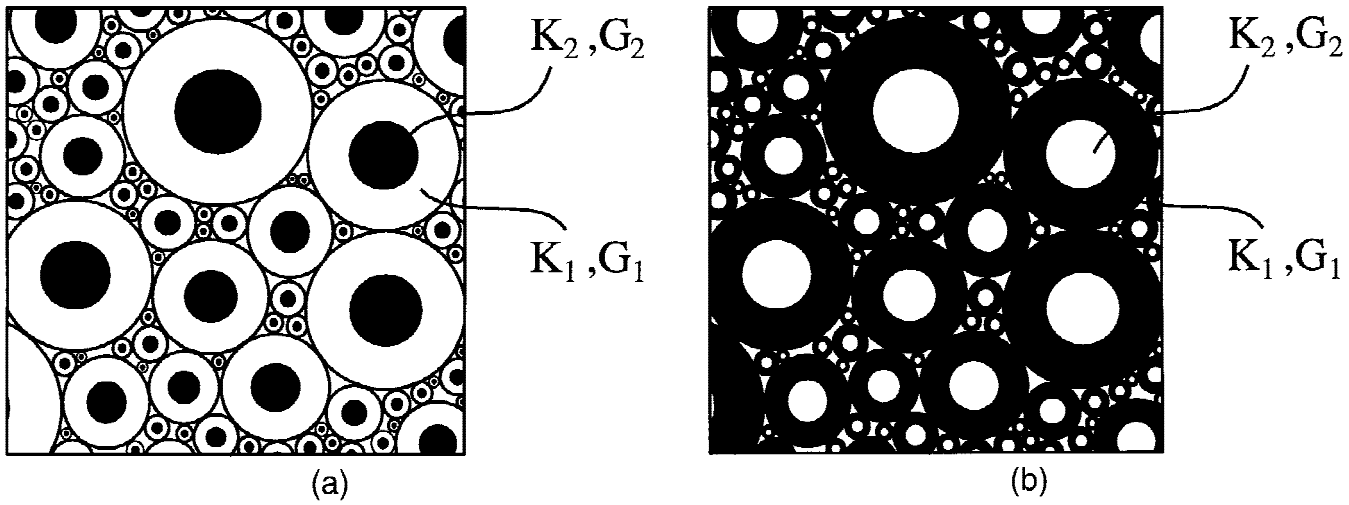

Fig. 3. Structures corresponding to the optimal HS (a) lower and (b) upper bounds, as discussed in the text.

nected. The HS bounds on K_e are realized by the same hierarchical laminates.[27]

To illustrate the utility of the bounds, we plot in Figs. 4 and 5 the one-point bounds and the two-point HS bounds on both K_e and G_e, respectively, for a *hypothetical* two-phase composite comprised of B_4C and aluminum as functions of the volume fraction of B_4C, ϕ_2. The HS bounds are relatively tight and considerably narrower than the one-point bounds. From these figures, we can estimate the error in the bounds given an error in volume-fraction measurements for this composite. This error depends on volume fraction and phase property values.

The HS bounds have been subsequently generalized by Walpole[16] by relaxing the condition that $K_2 \geq K_1$ and $G_2 \geq G_1$ and by treating N phase composites. Let the largest and smallest phase bulk moduli be denoted by K_{max} and K_{min}, respectively, and the largest and smallest phase shear moduli be denoted by G_{max} and G_{min}, respectively. Then K_e and G_e are bounded according to the relations

$$\left[\sum_{i=1}^{N}\phi_i(K^*_{min}+K_i)^{-1}\right]^{-1}-K^*_{min}\leq K_e \leq\left[\sum_{i=1}^{N}\phi_i(K^*_{max}+K_i)^{-1}\right]^{-1}-K^*_{max} \tag{7}$$

$$\left[\sum_{i=1}^{N}\phi_i(G^*_{min}+G_i)^{-1}\right]^{-1}-G^*_{min}\leq G_e \leq\left[\sum_{i=1}^{N}\phi_i(G^*_{max}+G_i)^{-1}\right]^{-1}-G^*_{max} \tag{8}$$

where

$$K^*_{min}=\frac{4}{3}G_{min} \tag{9}$$

$$K^*_{max}=\frac{4}{3}G_{max} \tag{10}$$

$$G^*_{min}=G_{min}\left[\frac{9K_{min}+6G_{min}}{6(K_{min}+2G_{min})}\right] \tag{11}$$

$$G^*_{max}=G_{max}\left[\frac{9K_{max}+6G_{max}}{6(K_{max}+2G_{max})}\right] \tag{12}$$

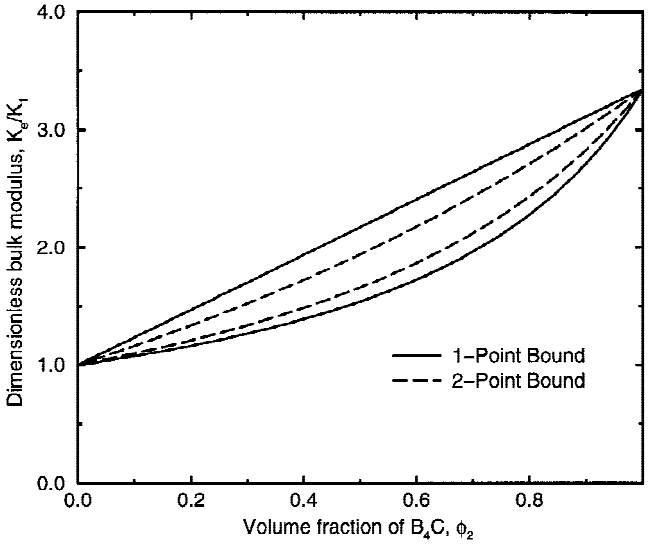

Fig. 4. One- and two-point HS bounds on the dimensionless effective bulk modulus versus volume fraction for a hypothetical two-phase composite composed of B_4C and aluminum.

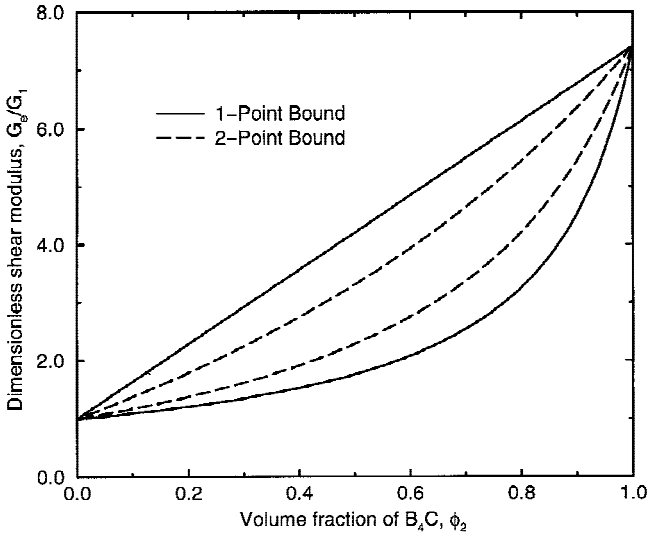

Fig. 5. One- and two-point HS bounds on the dimensionless effective shear modulus versus volume fraction for a hypothetical two-phase composite composed of B_4C and aluminum.

The multiphase bounds on K_e in Eq. (8) are also realizable by coated-sphere-type assemblages.[20,23] Again, the lower bound corresponds to structures in which the stiffer phase is the dispersed one and the upper bound corresponds to structures in which the stiffer phase is the connected one.

(3) Three-Point Bounds

Using minimum energy principles and admissible fields based upon the first few terms of the perturbation expression of the fields, Beran and Molyneux[17] and McCoy[18] derived three-point bounds on K_e and G_e, respectively, of two-phase composites. Subsequently, Milton and Phan-Thien[21] improved upon the McCoy shear-modulus bounds. The simplified form[19] of the three-point Beran–Molyneux bounds on K_e of isotropic two-phase composites is given by

$$\langle K\rangle - \frac{\phi_1\phi_2(K_2-K_1)^2}{\langle\tilde{K}\rangle + \frac{4}{3}\langle G^{-1}\rangle_\zeta^{-1}} \le K_e \le \langle K\rangle - \frac{\phi_1\phi_2(K_2-K_1)^2}{\langle\tilde{K}\rangle + \frac{4}{3}\langle G\rangle_\zeta} \tag{13}$$

and the three-point Milton–Phan-Thien bounds on G_e of isotropic two-phase composites are given by

$$\langle G\rangle - \frac{\phi_1\phi_2(G_2-G_1)^2}{\langle\tilde{G}\rangle + \Xi} \le G_e \le \langle G\rangle - \frac{\phi_1\phi_2(G_2-G_1)^2}{\langle\tilde{G}\rangle + \Theta} \tag{14}$$

where

$$\Xi = \frac{\left\langle \frac{128}{K} + \frac{99}{G}\right\rangle_\zeta + 45\left\langle\frac{1}{G}\right\rangle_\eta}{30\left\langle\frac{1}{G}\right\rangle_\zeta\left\langle\frac{6}{K}-\frac{1}{G}\right\rangle_\zeta + 6\left\langle\frac{1}{G}\right\rangle_\eta\left\langle\frac{2}{K}+\frac{21}{G}\right\rangle_\zeta} \tag{15}$$

$$\Theta = \frac{3\langle G\rangle_\eta\langle 6K+7G\rangle_\zeta - 5\langle G\rangle_\zeta^2}{6\langle 2K-G\rangle_\zeta + 30\langle G\rangle_\eta} \tag{16}$$

and, for any arbitrary property b,

$$\langle b\rangle_\zeta = b_1\zeta_1 + b_2\zeta_2 \tag{17}$$

$$\langle b\rangle_\eta = b_1\eta_1 + b_2\eta_2 \tag{18}$$

Where ζ_i and η_i are three-point microstructural parameters for phase i that are given by the following integrals:

$$\zeta_i = \frac{9}{2\phi_1\phi_2}\int_0^\infty\frac{dr}{r}\int_0^\infty\frac{ds}{s}\int_{-1}^1 d(\cos\theta)P_2(\cos\theta) \times\left[S_3^{(i)}(r,s,t) - \frac{S_2^{(i)}(r)S_2^{(i)}(s)}{\phi_i}\right] \tag{19}$$

$$\eta_i = \frac{5\zeta_i}{21} + \frac{150}{7\phi_1\phi_2}\int_0^\infty\frac{dr}{r}\int_0^\infty\frac{ds}{s}\int_{-1}^1 d(\cos\theta)P_4(\cos\theta) \times\left[S_3^{(i)}(r,s,t) - \frac{S_2^{(i)}(r)S_2^{(i)}(s)}{\phi_i}\right] \tag{20}$$

where P_2 and P_4 are the Legendre polynomials of order two and four, respectively, and θ the angle opposite the side of the triangle of length t. The quantity $S_3^{(i)}(r,s,t)$ is the probability of finding in phase i the vertices of a triangle with sides of lengths r, s, and t, when randomly inserted into the sample (see Fig. 2). That ζ_i must lie in the closed interval [0,1] implies that the bounds in Eq. (14) always improve upon the two-point HS bounds. The parameter η_i lies in the smaller interval $[5\zeta_i/21, (16 + 5\zeta_i)/21]$. Finally, $\zeta_1 + \zeta_2 = 1$ and $\eta_1 + \eta_2 = 1$.

Three-point bounds for the effective moduli of multiphase composites have been derived by Phan-Thien and Milton.[22] The number of three-point parameters to compute these bounds grows dramatically as the number of components increases. From a practical point of view, the amount of such required information quickly becomes unwieldy.

Table I. Experimental Data for Sample A

Parameter	Value
ϕ_1 (Al)	0.16
ϕ_2 (B_4C)	0.66
ϕ_3 (AlB_2)	0.02
ϕ_4 (Al_4BC)	0.16
K_e (GPa)	176
G_e (GPa)	125

III. Elastic Moduli Analysis

(1) Estimating the Moduli of the Al_4BC Phase

Four-phase composite samples that consist of B_4C, Al, AlB_2, and Al_4BC were fabricated by a process described elsewhere.[25,26] The AlB_2 and Al_4BC phases are reaction products that form during the heat treatment of the B_4C/Al composites. The volume fractions of the phases were measured by us, and K_e and G_e of the composites were determined at the Lawrence Livermore National Laboratory.¶ Table I summarizes these measurements for one such specimen, which we refer to as sample A.

Although the elastic properties of AlB_2 have long been known, Al_4BC is a new phase that was first identified during the fabrication of B_4C/Al composites.[29] We attempted to predict the elastic moduli of this new phase. We make several important observations and a plausible assumption to accomplish this task. First, the Al_4BC phase must have elastic moduli that lie between those of the most compliant phase 1 (aluminum) and the stiffest phase 2 (B_4C). Second, the B_4C and aluminum have phase contrast ratios that are moderate in values ($K_2/K_1 = 3.3$, $G_2/G_1 = 7.3$) and, importantly, are both connected phases. Third, together, the B_4C and aluminum occupy a majority of the fraction of space. For all of these reasons, we make the assumption that the effective properties lie midway between the HS upper and lower bounds in Eqs. (7) and (8). This is a reasonable first assumption based on our earlier discussion regarding the fact that the structures that realize the HS upper bound possess the most connected stiff phase, and the structures that attain the HS lower bound possess the most disconnected stiff phase. Under this assumption, we can use the measurements given in Table I, the phase moduli summarized in Table II, and the four-phase HS bounds to predict the moduli of Al_4BC phase. We find from Eqs. (7) and (8) that the moduli of the Al_4BC phase are given by

$$K_4 = 184\ \text{GPa} \tag{21a}$$

$$G_4 = 121\ \text{GPa} \tag{21b}$$

In a recent study, Pyzik and Beaman[30] experimentally determined the elastic moduli of the Al_4BC phase as

$$K_4 = 175\ \text{GPa} \tag{22a}$$

$$G_4 = 129\ \text{GPa} \tag{22b}$$

The prediction based on the HS bounds is in very good agreement with the experimental data for the Al_4BC phase, justifying the assumption that we made in our analysis as well as the general bounding approach that we use. However, this conclusion assumes that there are no experimental errors in the property and volume-fraction measurements.

¶We acknowledge the assistance of W. E. Snowden in the characterization of the elastic properties.

Table II. Known Elastic Phase Moduli

	K (GPa)	G (GPa)
Al	67.6	25.9
B_4C	226	192
AlB_2	170	120

The predictive capability of the most accurate structure–property relation to estimate phase properties is only as good as the accuracy of the known experimental measurements. An error analysis is actually a nontrivial task given the number of experimental measurements that characterize a multiphase composite. For the problem at hand, we use measurements of each phase volume fraction (ϕ_1, ϕ_2, ϕ_3, and ϕ_4), the elastic moduli of three of the four phases (K_1, G_1, K_2, G_2, K_3, and G_3), and the effective elastic moduli (K_e and G_e). To estimate the percent change from the zero-error estimate case given by Eq. (21), we assume that each measurement has a certain percentage error $\pm E$% relative to the values given in Tables I and II. In the case of volume-fraction measurements, we have the constraint that the sum of overall volume fractions must be unity.) E takes on three values: 0.5, 1, and 2. We also assume that errors among different measured quantities are uncorrelated; i.e., positive errors are just as likely as negative ones. Substitution of these measured values in our structure–property relations (simple averages of Eqs. (7) and (8)) yields the elastic moduli of the Al_4BC phase. For the cases $E = 0.5$, 1, and 2, we find that there is a 2.3%, 4.7%, and 11.1% change from Eq. (21), respectively. Thus, we conclude that, for our specific interpenetrating composite, the bounding approach is useful in predicting phase moduli. However, other situations may be problematical. For example, in the limit of zero volume fraction of a phase, any predictive approach breaks down. Moreover, predictive capability decreases as the contrast between the phase moduli becomes large.

(2) Estimating the Effective Moduli of a Three-Phase Composite Sample

A three-phase composite specimen (sample B) was fabricated consisting of aluminum (phase 1), B_4C (phase 2), and Al_4BC (phase 3). The two-dimensional optical microscope image of this sample is shown on the cover of this issue. The corresponding gray-scale digitized image (shown in Fig. 6) is obtained by simply thresholding the color and intensity of the original image. The size of the image is 602 pixels × 872 pixels and 1 pixel corresponds to 0.08 μm.

Available data for sample B are summarized in Table III. Unlike the first problem involving sample A, the effective moduli were not measured for sample B, because it was destroyed in dynamic loading experiments. However, the predictive capabilities of our approach already have been demonstrated at the level of two-point correlation function information for sample A. This gives us confidence that we can use the image of sample B to extract structural information, such as the phase volume fractions as well as additional information (three-point structural parameters ζ_2 and η_2) to obtain accurate estimates of the effective elastic moduli without always having to confirm the estimates via experimental measurements.

The parameters ζ_2 and η_2 are computed from the gray-scale digitized image (Fig. 6) using numerical and Monte Carlo techniques described by Smith and Torquato[31] and modified by Coker and Torquato.[32] Integration over r, s, and θ of Eqs. (19) and (20) via the Gaussian quadrature method is used to maintain sufficient integration accuracy while using a relatively small number of values of r, s, and θ. The values of $S_3(r,s,t)$ are evaluated at the vertices of the triangles specified by the Gaussian method and are then utilized in the integrands for immediate integration. In this way, the values of $S_3(r,s,t)$ need not be stored, which otherwise requires a large amount of computer memory. The term $S_2(r)\,S_2(s)$ in Eqs. (19) and (20) ensures the convergence of the integrals for large distances from the origin as well as to avoid singularities at the origin. Because the Gaussian quadrature points do not include the end points as a matter of course, this term can be omitted from the calculation. Furthermore, known symmetries of $S_3(r,s,t)$ and its long-range properties are also used to speed up the integration.

Fig. 6. Gray-scale digitized image of sample B (white region is Al phase, black region is B_4C phase, and gray region is Al_4BC phase). System size is 602 pixels × 872 pixels.

Table III. Structural Data Extracted from the Digitized Image of Sample B

Parameter	Value
ϕ_{Al}	0.31
ϕ_{B_4C}	0.64
ϕ_{AlB_2}	0.05
ζ_2	0.53
η_2	0.53

The integration method is applied to the gray-scale digitized image of the B_4C/Al cermet, and periodic boundary conditions are used. The algorithm is crudely run first with low integration resolution (a relatively small number of quadrature points) to define the upper ranges of r and s that should be used. During the actual evaluation of ζ_2 and η_2, the domains of integration for r and s are divided in three and four subregions, respectively, each having 48 quadrature points. The domain for θ, on the other hand, is not divided in smaller regions and is comprised of 32 quadrature points. The quantities of ζ_2 and η_2 have the values of 0.533 and 0.531, respectively.

Using the volume fractions, the three-point parameters ζ_2 and η_2, and the phase properties, we now estimate K_e and G_e, using the aforementioned one-, two-, and three-point bounds. The one- and two-point bounds of the three-phase composite sample are evaluated simply by substituting appropriate information into Eqs. (1), (2), (7), and (8). For the three-point bounds, to avoid computing the more-complex multiphase bounds, we instead compute the two-phase, three-point bounds given by Eqs. (13) and (14) by assuming that the ceramic phases (B_4C and Al_4BC) can be treated as an effective medium. This is a superb approximation, because the bounds on the elastic moduli of this effective phase are extremely tight:

$$221.6 \text{ GPa} \leq K_e \leq 221.7 \text{ GPa}$$

$$186.1 \text{ GPa} \leq G_e \leq 186.3 \text{ GPa}$$

The ceramic phases can now be treated as one "homogenized" phase. Because the stiffer phase is the connected phase, the upper bounds provide the better estimates of the elastic moduli of the effective medium. Utilizing these approximations and treating the material as a two-phase composite, we have evaluated the three-point bounds in Eqs. (13) and (14) on the effective moduli of the composite. We also compute corresponding two-phase one- and two-point bounds by assuming that the ceramic phases can be viewed as one effective homogeneous phase.

All of the aforementioned evaluations of the bounds are summarized in Table IV. The one-point bounds are far apart. The HS bounds are narrower, but the three-point bounds are quite restrictive, yielding the bounds

$$146.6 \text{ GPa} \leq K_e \leq 155.7 \text{ GPa}$$

$$94.8 \text{ GPa} \leq G_e \leq 108.2 \text{ GPa}$$

The bounds on K_e determine the effective bulk modulus to within ~6%, and the bounds on G_e determine the effective shear modulus to within ~13%.

IV. Concluding Remarks

We have presented a comprehensive rigorous analysis of the elastic properties and structure of interpenetrating B_4C/aluminum multiphase composites. Four-phase composite samples were fabricated consisting of B_4C, aluminum, and two reaction-product phases, AlB_2 and Al_4BC. By utilizing experimentally measured values of the phase volume fractions, effective elastic moduli, and phase properties of three phases of the four-phase composite (sample A), we predicted accurately the property of the fourth phase (Al_4BC), using two-point bounds. A three-phase composite (sample B) was also fabricated consisting of aluminum (phase 1), B_4C (phase 2), and Al_4BC (phase 3), in which the effective elastic moduli were not measured. By extracting three-point microstructural parameters from the two-dimensional image of the sample, we accurately predicted the effective bulk and shear moduli of sample B using rigorous three-point bounds.

Acknowledgments: S. T., C. L. Y. Y., and M. D. R. gratefully acknowledge the support of the Air Force Office of Scientific Research under Grant No. F49620-96-1-0182. I. A. A. and D. L. M. also acknowledge the support of the Air Force Office of Scientific Research under Grant No. F49620-93-1-0259.

Table IV. Bounds on K_e and G_e for Sample B

	K_e (GPa)	G_e (GPa)
One-point upper bound (three phases)	175.1	138.1
One-point upper bound (two phases)	174.9	137.5
Two-point upper bound (three phases)	161.2	116.7
Two-point upper bound (two phases)	160.9	116.3
Three-point upper bound (two phases)	155.7	108.2
Three-point lower bound (two phases)	146.6	94.8
Two-point lower bound (two phases)	141.0	85.2
Two-point lower bound (three phases)	140.9	85.0
One-point lower bound (two phases)	131.2	64.6
One-point lower bound (three phases)	130.7	64.5

†Two phases means that the ceramic phases are treated as a single homogenized phase. As discussed in the text, this is an extremely accurate estimate.

References

[1]J. C. Maxwell, *Treatise on Electricity and Magnetism*, 1st ed. Clarendon Press, Oxford, U.K., 1873.
[2]Lord Rayleigh, "On the Influence of Obstacles Arranged in Rectangular Order upon the Properties of Medium," *Philos. Mag.*, **34**, 481–502 (1892).
[3]A. Einstein, "Eine neue Bestimmung der Moleküldimensionen," *Ann. Phys.* (*Leipzig*), **19**, 289–306 (1906).
[4]M. J. Beran, *Statistical Continuum Theories*. Wiley, New York, 1968.
[5]D. K. Hale, "The Physical Properties of Composite Materials," *J. Mater. Sci.*, **2**, 2105–41 (1974).
[6]R. M. Christensen, *Mechanics of Composite Materials*. Wiley, New York, 1979.
[7]S. Torquato, "Random Heterogeneous Media: Microstructure and Improved Bounds on Effective Properties," *Appl. Mech. Rev.*, **44**, 37–76 (1991).
[8]S. Torquato, "Morphology and Effective Properties of Disordered Heterogeneous Media," *Int. J. Solids Struct.*, **35**, 2385–406 (1998).
[9]S. Torquato, "Exact Expression for the Effective Elastic Tensor of the Disordered Composites," *Phys. Rev. Lett.*, **79**, 681–84 (1997).
[10]K. C. Nunan and J. B. Keller, "Effective Elasticity Tensor of a Periodic Composite," *J. Mech. Phys. Solids*, **32**, 259–80 (1984).
[11]R. Hill, "Self-Consistent Mechanics of Composite Materials," *J. Mech. Phys. Solids*, **13**, 213–22 (1965).
[12]B. Budiansky, "On the Elastic Moduli of Some Heterogeneous Materials," *J. Mech. Phys. Solids*, **13**, 223–27 (1965).
[13]R. Hill, "The Elastic Behavior of a Crystalline Aggregate," *Proc. R. Soc. London A*, **65**, 349–54 (1952).
[14]B. Paul, "Prediction of Elastic Constants of Multiphase Materials," *Trans. Metall. Soc. AIME*, **218**, 36–41 (1960).
[15]Z. Hashin and S. Shtrikman, "A Variational Approach to the Theory of the Elastic Behavior of Multiphase Materials," *J. Mech. Phys. Solids*, **11**, 127–40 (1963).
[16]L. J. Walpole, "On Bounds for the Overall Elastic Moduli of Inhomogeneous Systems I.," *J. Mech. Phys. Solids*, **14**, 151–62 (1966).
[17]M. J. Beran and J. Molyneux, "Use of Classical Variational Principles to Determine Bounds for the Effective Bulk Modulus in Heterogeneous Media," *Q. Appl. Math.*, **24**, 107–18 (1966).
[18]J. J. McCoy, "On the Displacement Field in an Elastic Medium with Random Variations of Material Properties," *Recent Adv. Eng. Sci.*, **5**, 235–54 (1970).
[19]G. W. Milton, "Bounds on the Electromagnetic, Elastic, and Other Properties of Two-Component Composites," *Phys. Rev. Lett.*, **46**, 542–45 (1981).
[20]G. W. Milton, "Concerning Bounds on the Transport and Mechanical Properties of Multicomponent Composite Materials," *Appl. Phys.*, **A26**, 125–30 (1981).
[21]G. W. Milton and N. Phan-Thien, "New Bounds on the Effective Moduli of Two-Component Materials," *Proc. R. Soc. London A*, **380**, 305–31 (1982).
[22]N. Phan-Thien and G. W. Milton, "New Third-Order Bounds on the Effective Moduli of *n*-Phase Composites," *Q. Appl. Math.*, **41**, 59–74 (1983).
[23]K. A. Lurie and A. V. Cherkaev, "The Problem of Formation of an Optimal Multicomponent Composite," *J. Opt. Th. Appl.*, **46**, 571–89 (1985).
[24]D. C. Halverson, A. J. Pyzik, and I. A. Aksay, "Boron Carbide–Aluminum and Boron Carbide–Reactive Metal Cermets," U.S. Pat. No. 4 605 440, Aug. 12, 1986.
[25]A. J. Pyzik and I. A. Aksay, "Multipurpose Boron Carbide–Aluminum Composite and Its Manufacture via the Control of the Microstructure," U.S. Pat. No. 4 702 770, Oct. 27, 1987.
[26]A. J. Pyzik and I. A. Aksay, "Microdesigning of B_4C–Al Cermets"; pp. 269–80 in *Processing of Ceramic and Metal Matrix Composites*. Edited by H. Mostaghaci. Pergamon Press, New York, 1989.
[27]K. A. Lurie and A. V. Cherkaev, "The Problem of Formation of an Optimal Multicomponent Composite," *J. Opt. Th. Appl.*, **46**, 571–78 (1985).
[28]G. A. Francfort and F. Murat, "Homogenization and Optimal Bounds in Linear Elasticity," *Arch. Ration. Mech. Anal.*, **94**, 307–34 (1986).
[29]M. Sarikaya, T. Laoui, D. L. Milius, and I. A. Aksay, "Identification of a New Phase in the Al–C–B Ternary by High-Resolution Transmission Microscopy"; pp. 168–69 in *Proceedings of 45th Annual Meeting of EMSA*. Edited by G. W. Bailey. San Francisco Press, San Francisco, CA, 1987.
[30]A. J. Pyzik and D. R. Beaman, "Al–B–C Phase Development and Effects on Mechanical Properties of B_4C/Al-Derived Composites," *J. Am. Ceram. Soc.*, **78**, 305–12 (1995).
[31]P. A. Smith and S. Torquato, "Computer Simulation Results for Bounds on the Effective Conductivity of Composite Media," *J. Appl. Phys.*, **65**, 893–900 (1989).
[32]D. A. Coker and S. Torquato, "Extraction of Morphological Quantities from a Digitized Image," *J. Appl. Phys.*, **77**, 6087–99 (1995). □